Staircased Wire Monopole Antennas used to evaluate Finite-Different Time-Domain Models

Prepared by:
Jaron Volk
Samantha Wehrkamp

Faculty Advisors:
Dr. Thomas Montoya
REU Site Director, Electrical Engineering Department

Dr. Alfred Boysen
Professor, Department of Humanities

Programs Information:
National Science Foundation
Grant NSF #1359476

Research Experience for Undergraduates
Summer 2014

South Dakota School of Mines and Technology
501 E Saint Joseph Street
Rapid City, SD 57701

TABLE OF CONTENT

Abstract

This work presents results of research on a variety of staircase, i.e., repeated right angle bends, wire monopole antennas in order to assess the performance and accuracy of finite-difference time-domain (FDTD) models. The FDTD numerical method is used for electromagnetic simulations of many problems and geometries, e.g., wire antennas and ground penetrating radars. A vector network analyzer is used to measure the S-parameter S_{11} and input impedance of the antennas. This data allows the change in the apparent velocity of wave propagation along the experimental staircase wire monopole antennas to be examined and compared to results obtained from FDTD models. Two different techniques for constructing staircase monopole antennas were analyzed and compared to that of straight monopole antennas to access the accuracy of the results.

The soldered staircase monopole wire antennas that were tested provided data that was directly comparable to that of the same height and gauge monopole straight antenna. This information provides proof that the soldered 90° staircase antennas constructed were indeed successful in modeling a similar straight antenna. In the case of larger gauge (smaller radius) wire antennas bent using a plastic mold in attempt to perfectly model a 90° angled staircase, the results were not directly comparable. Therefore, construction by bending using a plastic mold is not the preferred fabrication method.

1. Introduction

Finite-Different Time-Domain (FDTD) is a numerical analysis technique used for electromagnetic simulations of many problems and geometries. FDTD uses a grid-based differential numerical modeling method to break a computational domain into cells, about which electric and magnetic field vector components are distributed. The grid model is useful when considering FDTD is a time-domain method and can cove a wide frequency range with a single simulation run.

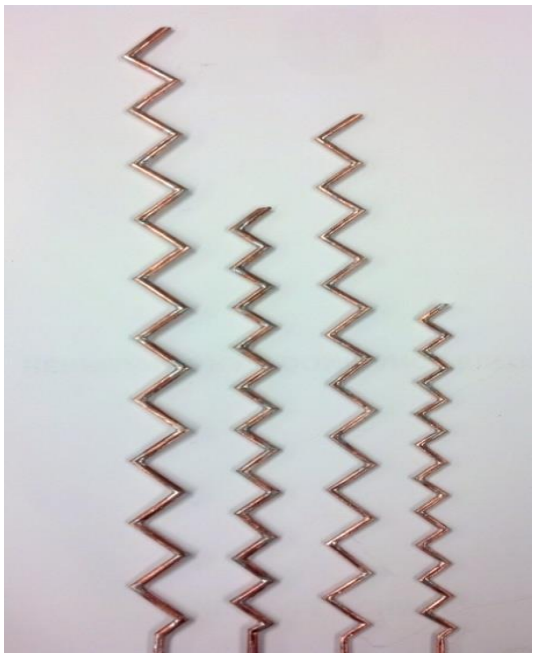

Figure 1: Experimental stairecase antennas showing a range of Δs dimensions in 12-14AWG

Experimental staircase antennas (repeated 90° bends, Figure 1), which were earlier compared to an FDTD model that simply set electric field components to zero within the wire, have not produced results that were in a direct relationship of one

another. Incorporating the radius of the wire and variation of the fields as variables into the model can further improve the similarities of the staircase antennas and the representative FDTD model. In order to construct a working mathematical model, more data must be collected from a range of staircase antenna simulations.

To accomplish this goal, antennas must be fabricated with a step size (Δs) calculated to meet requirements, perfect 90° angles, and a large enough height for comprehensible results. The constructed monopole antennas (Figure 1) are tested on a ground place with conductive properties to produce a mirroring effect. This mirroring effect produces radiation patterns identical to a center-fed dipole antenna and an impedance that is half that of a dipole. Data collected for the monopole staircase copper antennas will then be used for direct comparison of improved FDTD staircase models.

2. Broader Impact

Every year around 10,000 civilian casualties are a direct result of inadvertent detonation of buried landmines. The United Nations estimates the number of buried landmines to be about 100 million. Continuous research on this issue is crucial in order to counteract each new development in mine technology. Ground-penetrating radar (GPR) has proven to be one of the most promising techniques for detection of landmines. Therefore, further work on analyzing the possibilities of GPR is imperative.

Numerical methods, such as the finite-difference time-domain, (FDTD) method, can be used to perform full electromagnetic simulations of ground-penetrating radars for landmine detection. All elements that are important to the problem can be included in the simulation, such as, the details of the detector, the peculiarities of the mine, the electrical properties of the ground including dispersion, inhomogeneities, and surface roughness. These simulations can be used to test new concepts for detectors and to optimize the performance of the components in existing detectors.

Since the FDTD method is to be used for electromagnetic simulations of many problems and geometries, being able to adapt the numerical method to fit different situations is important. Experimental testing to improve or discredit the FDTD method techniques must be conducted in order to understand errors and make improvements.

3. Procedure

Materials

Solid cylindrical copper wire in gauges ranging from 12 - 14 AWG were used as the body for every antenna tested. Other metals were considered; however, since copper is both effective and reasonably inexpensive, it proved to be the most logical choice. The only other material present in the constructed antennas was solder. Solder is composed of lead and tin; both have different electrical properties then copper. However, since lead and tin are still highly conductive materials and a minimal amount of solder is used on the finished antenna, the differences in electrical properties were negligible.

Equipment

When forming 90° joints in copper wire, gauges 12 through 14AWG, the main piece of equipment used was a soldering iron. Other small tools such as wire cutters, files, and clamps were all used to prepare the wire to be soldered. A Weller WES51 soldering station was used as the heat source when constructing all soldering joints.

Other equipment was also used in the testing of the antennas. A vector network analyzer (Agilent VNA-4396B) that was connected to an S-Parameter test set (Agilent-85046A) was used to gather S_{11} data verse frequency A 3.5mm cable set and a 3.5mm calibration set was used with the vector network analyzer (VNA).

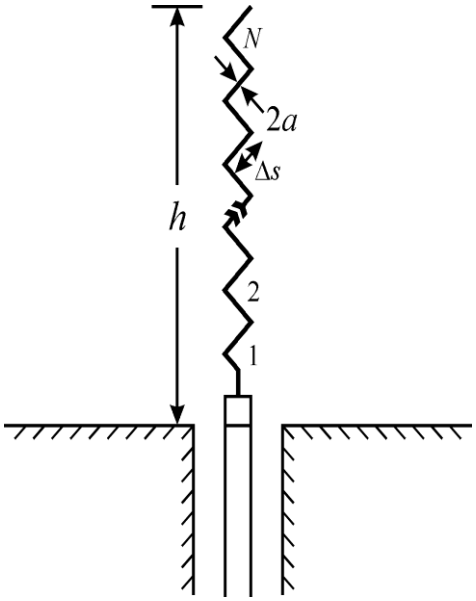

Figure 2:

Fabrication Procedures

For cylindrical copper wires with gauges 12 through 14 AWG, small predetermined staircase step sections of length Δs were cut using a wire cutter and filed down to 45° angles at both ends. Once a minimum of 20 sections were created, two of them could be soldered together in order to create the needed 90° angle in the staircase antenna. This connection of two sections, comprise one step (N) out of an antenna (Figure 2). A vertical section of copper wire, that is half the length of Δs, is added at the bottom of the antenna. Upon completion of soldering, the vertical tip of the monopole antennas were mounted at the center of a 104 x 92 cm ground plane on the center conductor of a SMA 3.5mm bulkhead connector.

3. Testing & Results

The next step in acquiring results was to calibrate the vector network analyzer (Agilent VNA-4396B) that was connected to an S-Parameter (S_{11}) test set (Agilent-85046A). The calibration was done to remove the effects of the two 4ft lengths of 3.5mm cables that connected the VNA to the antenna. These cables were necessary to reach the center of the 104 x 92cm ground plane. Note that the ground plane is surrounded by anechoic foam, shown in Figure 3, to lessen unwanted signals from the surroundings. First, we set the desired frequency range (20- 1820 MHz), and number of data points (601) which resulted in a frequency step size of 3MHz. Next, the calibration procedure involved attaching three known loads and using the known data to match the data readings accordingly; this removed the effects of the cables and connectors. With the calibration complete we were capable of calculating accurate S_{11} data for each antenna and the input impedance (Z_{in}) as seen by the source for each antenna connected.

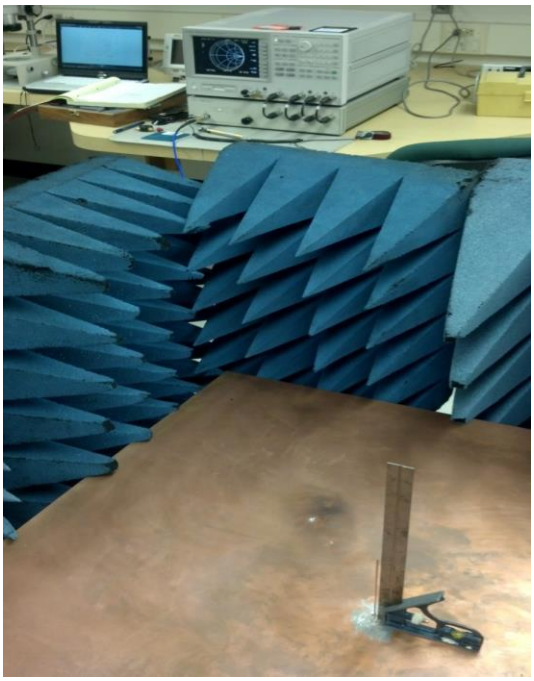

Figure 3: Picture of a straight monopole antenna connected to the VNA

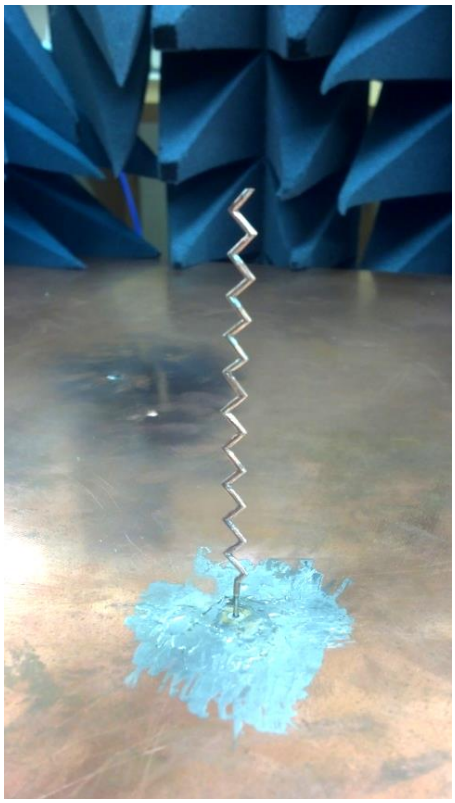

Figure 4: 12AWG_8.2mm step size staircase antenna mounted (soldiered) to the 104x92mm ground plane

Once the calibration was done, we connected the cable from the VNA to the 3.5mm SMA bulkhead connector located at the center of the ground plane. Then, we needed to remove the effects of the SMA bulkhead connector in order to measure the true S_{11} of the antennas. This was done by first placing the VNA in Smith Chart display mode. Then, a flat piece of metal was placed on the ground plane and slid toward the center bulkhead connector pin, ultimately making contact, and creating a short circuit. The electric delay on the VNA was then adjusted until the trace displayed became a dot on the left hand side, indicating a short. For the first test, the necessary electrical delay was 48.75ps. The metal plate was then removed.

Next, the averaging factor for VNA was set at 8 (i.e., data is a rolling average of the last eight measurements) The test was allowed to reach a steady state. Then, the S11 data was saved ASCII format and graphics data file of the VNA display was saved after setting the format to Smith chart.

$$Z_{in} = (Z_0)\frac{1+S_{11}}{1-S_{11}}$$

Figure 5: Equation used to calculate impedance seen by the source ()

The S_{11} data, collected for the frequency range 20MHz – 1.82GHz, was then used in the equation of figure 5, to calculate (Z_{in}). The real and imaginary parts of Z_{in} were graphed versus frequency as shown in Figures 6-13. The Z real values are graphed in blue and the Z_imaginary parts are graphed in red. All graphs are placed in pairs, starting with the staircase antenna and then followed by the straight antenna of the same height. It is expected that the curves for the staircase antenna

will be similar compared to the staircase wire monopoles. The Smith Charts for the antennas are found in the Appendix Figure 1-8.

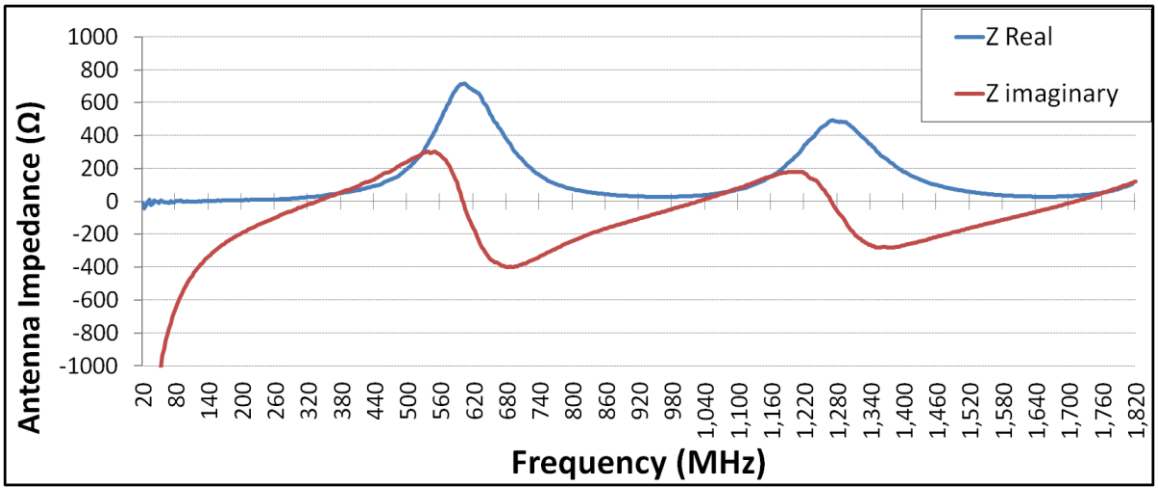

Figure 6: Impedance data from 12AWG and Δs size 12mm staircase antenna

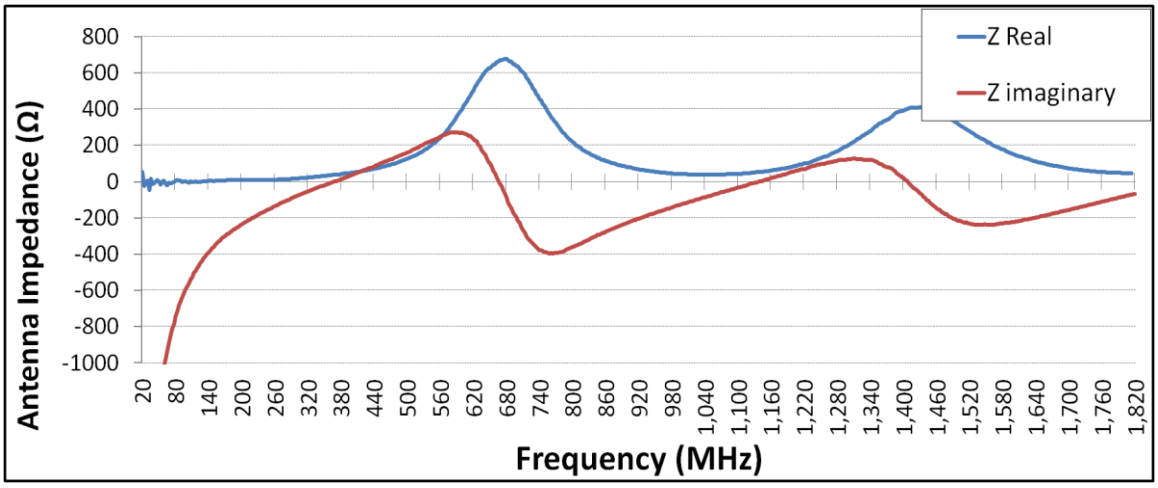

Figure 7: Impedance data from 12AWG and Δs size 192mm straight monopole antenna

Figure 4 shows the impedance for a 12AWG copper wire with a Δs size of 12 mm. The antenna also had 10N, which made for a total height of 192mm. Figure 5 is showing a 12AWG wire with the same height as the antenna from Figure 4 but is a straight monopole. As you can see these two antennas have a very similar curve pattern even though the one in figure 4 is a staircase antenna and the one in figure 5 is a straight monopole antenna. However, the impedance curve for the staircase

antenna are shifted to lower frequencies The comparison of the first resonant point where Z_Imaginary = 0, is listed in Table 1 below.

Shown in figure 7-8 are the rest of the staircase and straight antennas impedance data vs. frequency paired up to show the visual comparison.

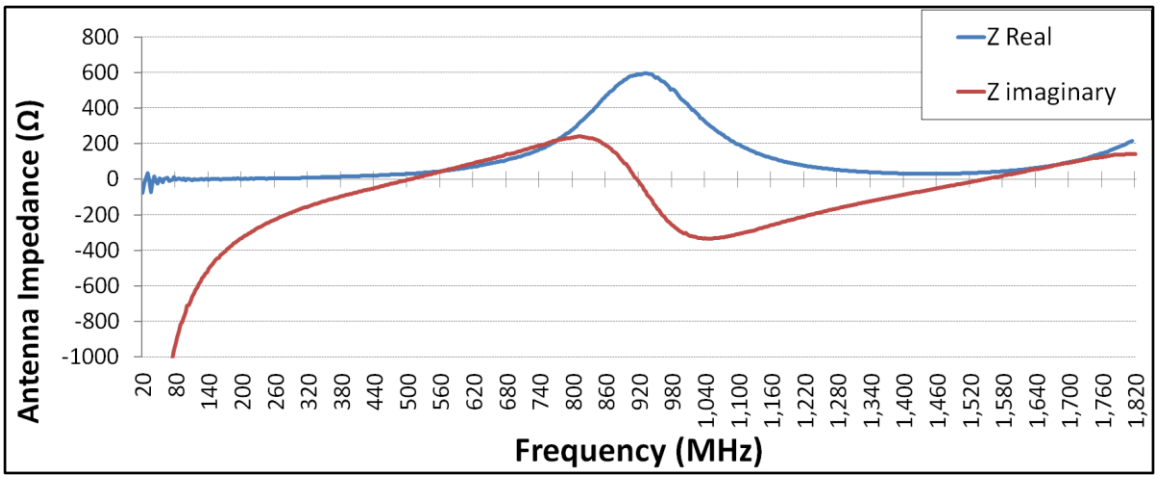

Figure 8: Impedance data from staircase antenna with 12AWG wire Δs of 8.2mm

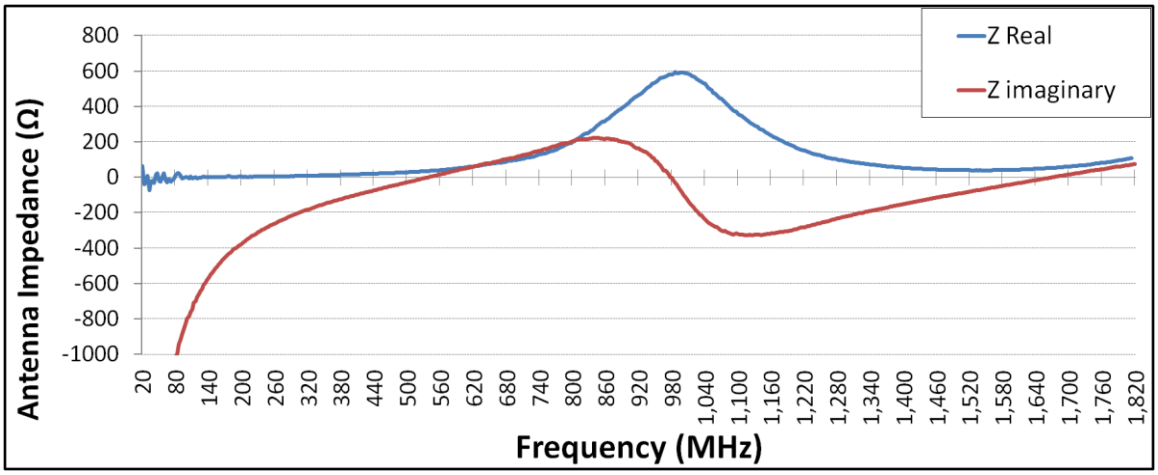

Figure 9: Impedance data from monopole antenna with 12AWG wire and a height of 130mm

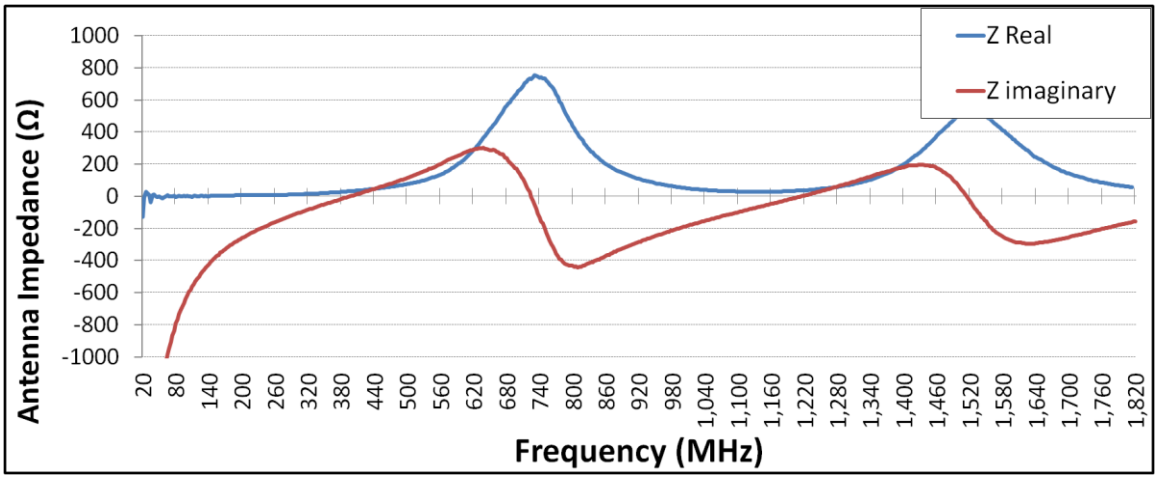

Figure 10: Impedance data from staircase antenna with 14AWG wire Δs of 10mm

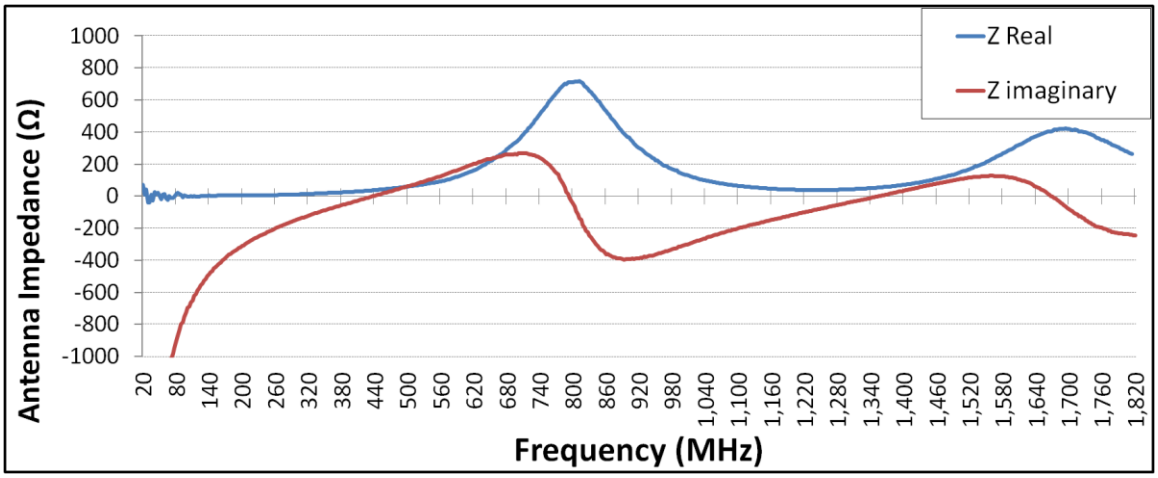

Figure 11: Impedance data from staircase antenna with 12AWG wire and a height of 161mm

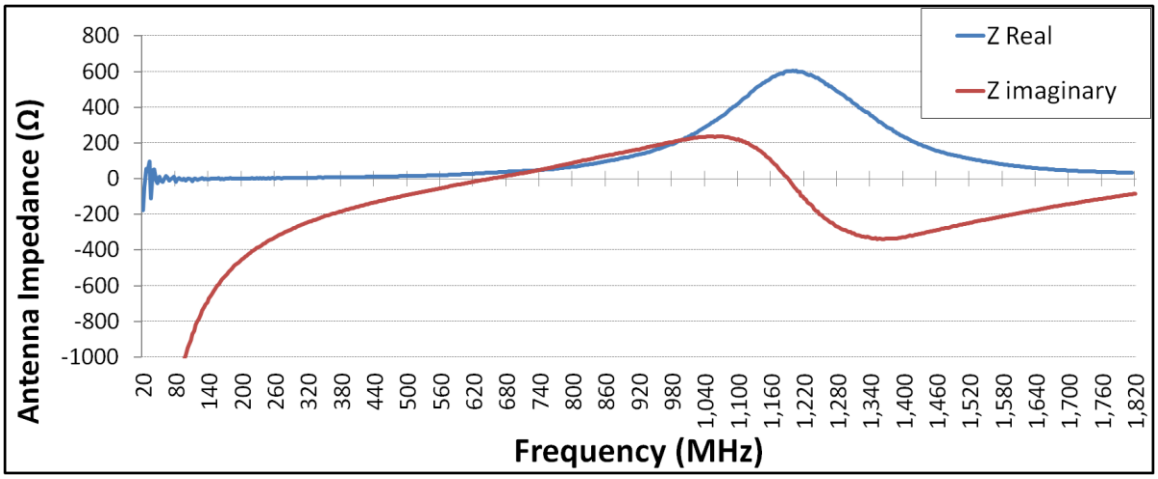

Figure 12: Impedance data from staircase antenna with 14 AWG wire Δs of 6.2mm

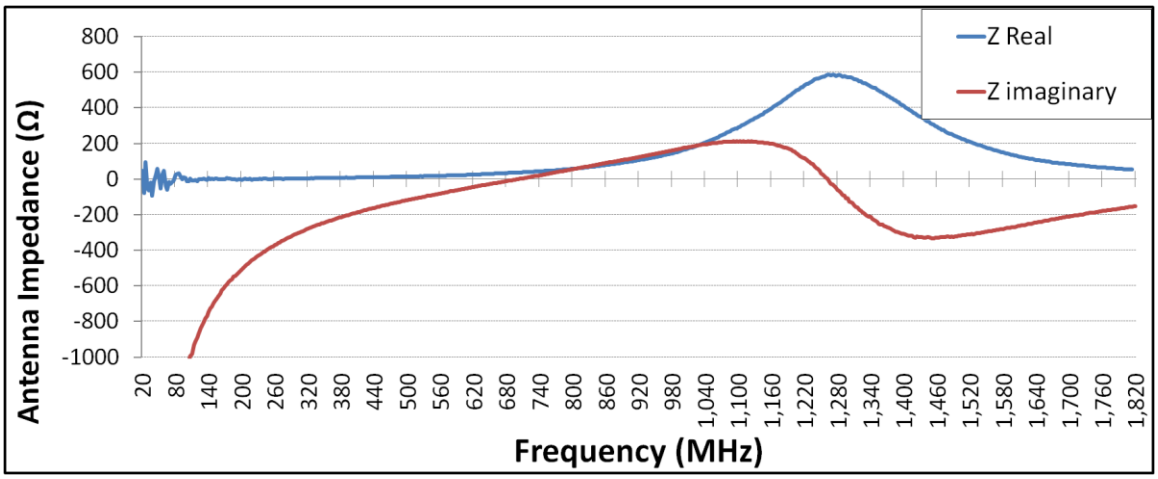

Figure 13: Impedance data from staircase antenna with 14AWG wire and a height of 8.2mm

Data Analysis						
	Height (mm)	Frequency (Hz)	S_{11}_Real	S_{11}_Imaginary	Z_Real (Ω)	Z_Imaginary (Ω)
12AWG_12mm Staircase Antenna	192.088	335	-0.256094	0.002899	29.61	0
12AWG_192mm Straight Antenna	192.088	368	-0.134224	0.007875	38.16	0
12AWG_8.2mm Staircase Antenna	130.175	506	-0.22664	0.017305	31.507	0
12AWG_130mm Straight Antenna	130.175	539	-0.16886	0.008204	35.16	0
14AWG_10mm Staircase Antenna	161.925	398	-0.217398	0.025243	32.107	0
14AWG_161mm Straight Antenna	161.925	440	-0.140509	0.032711	37.608	0
14AWG_6.2mm Staircase Antenna	100.013	653	-0.190826	0.007866	33.971	0
14AWG_100mm Straight Antenna	100.013	704	-0.149108	0.010403	37.0169	0

Table 1: Data comparison of staircase antennas vs. straight monopole antenna of the same height (h)

After looking at the first resonant point on each graph and comparing the Z_Real values, we notice that the traces for straight antenna graphs are slightly shifted to the right (higher frequencies) compared to the comparable staircase antennas. This is due to the shorter amount of wire for the same height wire. As this is expected, this data validates our results. This information is also located in Table 1 above.

5. Discussion

Ranges of staircase antennas were tested with 12 to 14AWG and with Δs 6.2 to 12mm. This data is validated comparison with straight monopole antennas of the same height. Four Δs of antennas were tested and the results are located in Table 1. This information shows the comparison of frequency, and Z_Real between the two types (staircase and straight) of the same height.

The input impedance $Z_{in,}$ as seen a source, is graphed for the antennas (Figure 6-13). As you can see, Z_{in} for each of the antennas that are the same height have a similar curve pattern. However, the curves for the staircase antennas are shifted to lower frequencies. This result is expected and is typical of staircased antennas verse straight antennas of the same height. Therefore, these graphs also validate the data from the staircase antennas. When looking at the graph pattern of the staircase antennas verse straight antennas, note that that the straight antenna graph pattern is shifted to the right of the staircase antennas. This is also noted in table one as the resonant point for each of the straight antennas is at a higher frequency then the staircase antenna.

Dr. Montoya will use these results in the development of accurate FDTD models for staircase wire antenna. In addition this will aid in the development of accurate FDTD models for right angle thin wire bends in general.

6. Conclusion

The test data for staircase antennas constructed from 12-14AWG with step sizes $\Delta s = 6.2 - 12$mm will be used to assess the performance and accuracy of FDTD wire antenna models by Dr. Thomas Montoya. Once a working FDTD model is developed that can represent a wide range of staircase antennas (AWG and Δs), then practical electromagnetic simulations can be produced for many problems and geometries, such as wire antennas and ground penetrating radar.

References

1. Montoya, T. P. & Smith, G. S. (2013, April). Modeling Staircased Thin Wires using the FDTD Method. *SD Academy of Science 98th Annual Meeting*. Lecture conducted from Augustana College, Sioux Falls, SD.

2. Montoya, T. P. & Smith, G. S. (2013, July). Using the FDTD method to Accurately Model Stair cased Thin Wires. *USNC/URSI National Radio Science Meeting*. Lecture conducted from Chicago, IL.

3. Montoya, T. P. & Swiatkowski, M. J. (2000, July). Normal Mode Bent Wire Antennas. *USNC/URSI National Radio Science Meeting*. Lecture conducted form Salt Lake City, UT.

4. Montoya, T. P. & Smith, G. S. & Maloney, J. G. (1998, April). Electromagnetic simulation of ground-penetrating radars for mine detection. *SPIE Conf. on Detection and Remediation Tech. for Mines and Minelike Targets III*. Lecture conducted from Orlando, FL.

5. Montoya, T. P. & Smith, G. S. (1997, July). Mine Detection using Vee Dipoles in a Short-Pulse Ground Penetrating Radar. *1997 North American Radio Science Meeting (URSI).* Lecture conducted from Montreal, Canada.

6. Boutros-Ghali, B. (1994, September). The land mine crisis. *Foreign Affairs*, 73, 8-13.

7. Morrison, P. & Tsipis, K. (1997, October). New hope in the minefields. Technology Review, 38-47.

Acknowledgments

The funding for this research came from the National Science Foundation (EEC-1359476). Thanks to advisor and REU site director Dr. Thomas Montoya for his direction and guidance, Professor of English Dr. Alfred Boysen for his critique in writing and speaking, and special thanks to all of the faculty and staff at SDSM&T.

Appendix

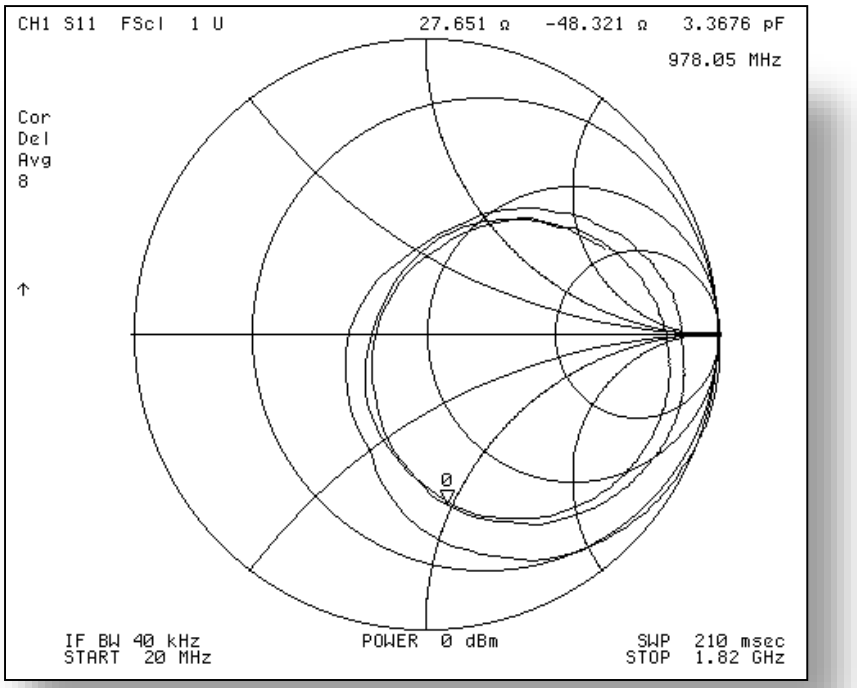

Appendix Figure 1: Smith chart data for 12AWG_12mmStepSize

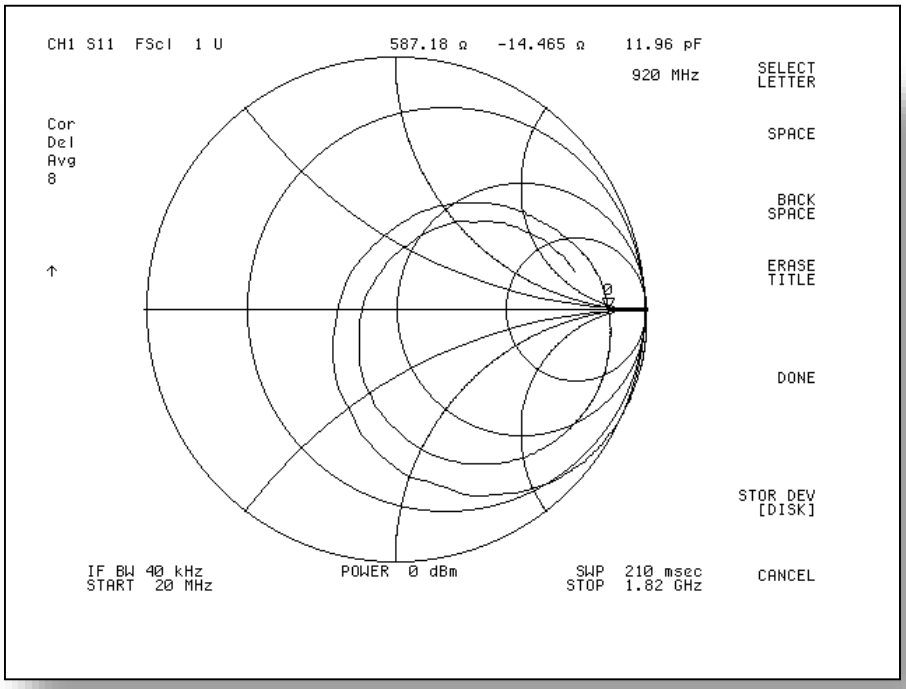

Appendix Figure 2: Smith chart data for 12AWG_8.2mmStepSize

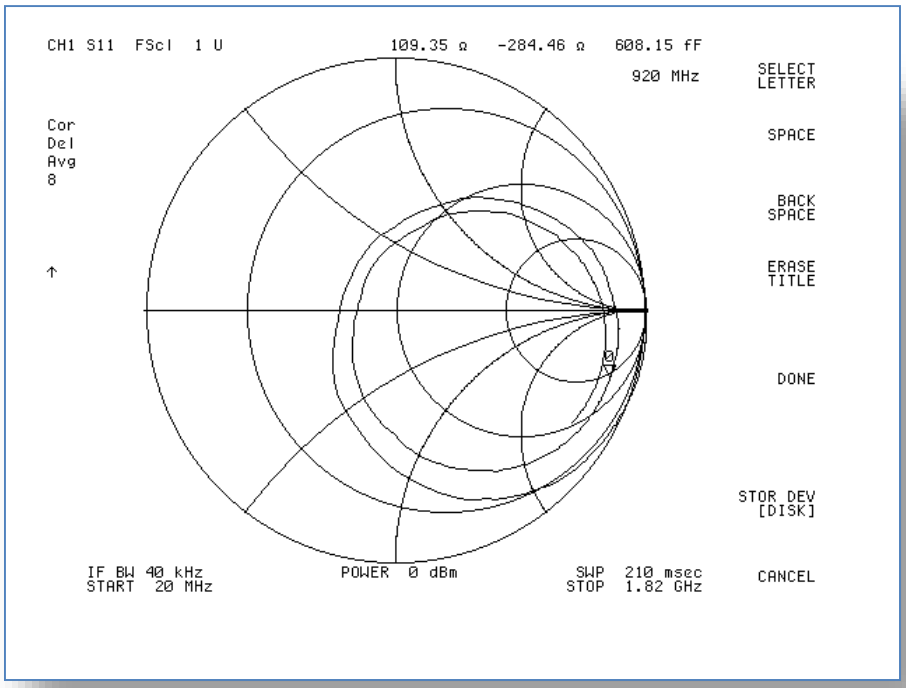

Appendix Figure 3: Smith chart data for 14AWG_10mmStepSize

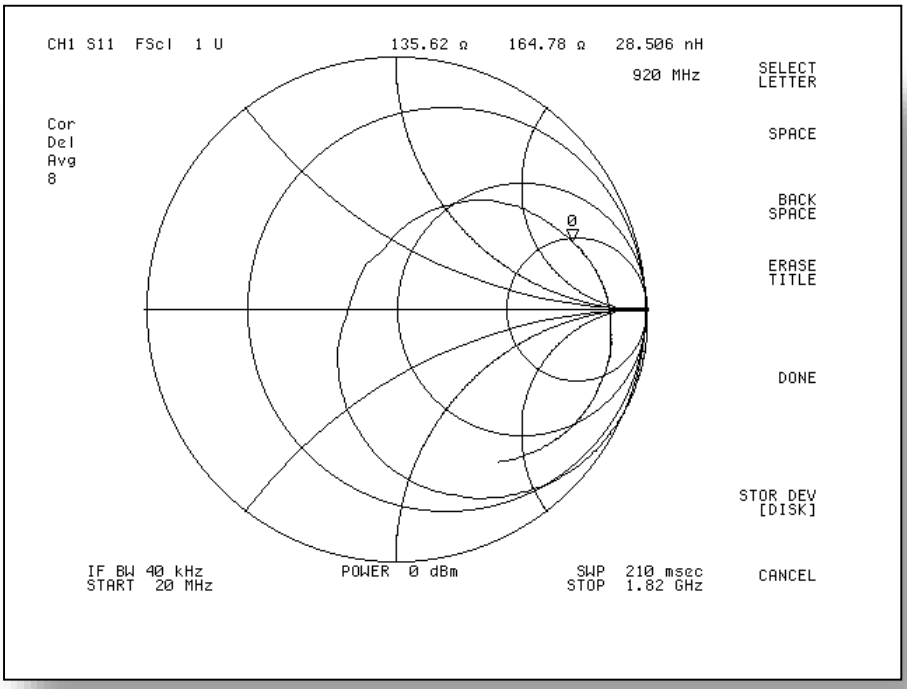

Appendix Figure 4: Smith chart data for 14AWG_6.2mmStepSize

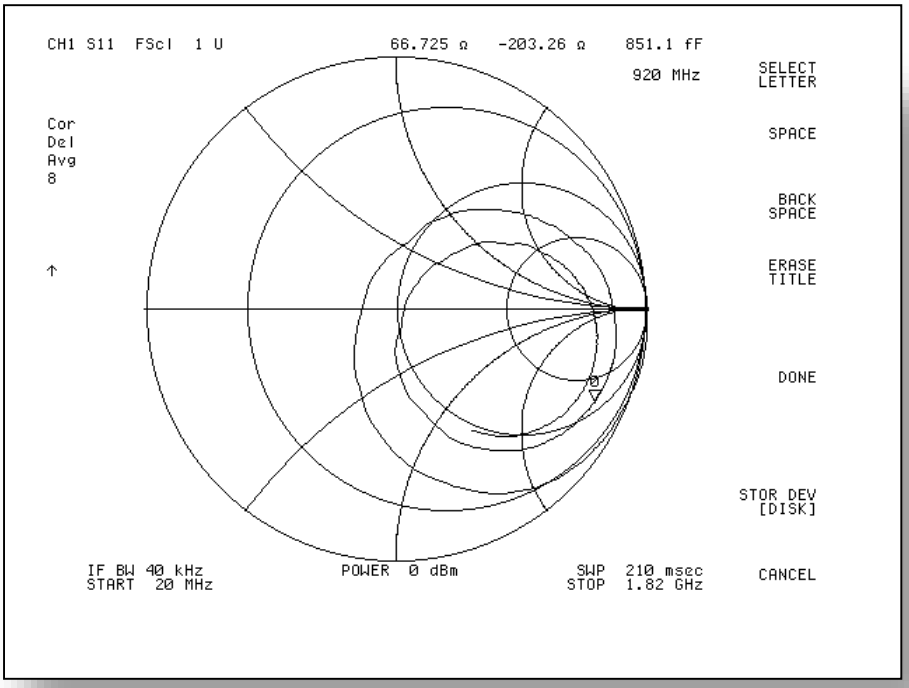

Appendix Figure 5: Smith chart data for 12AWG_192mm Straight monopole antenna

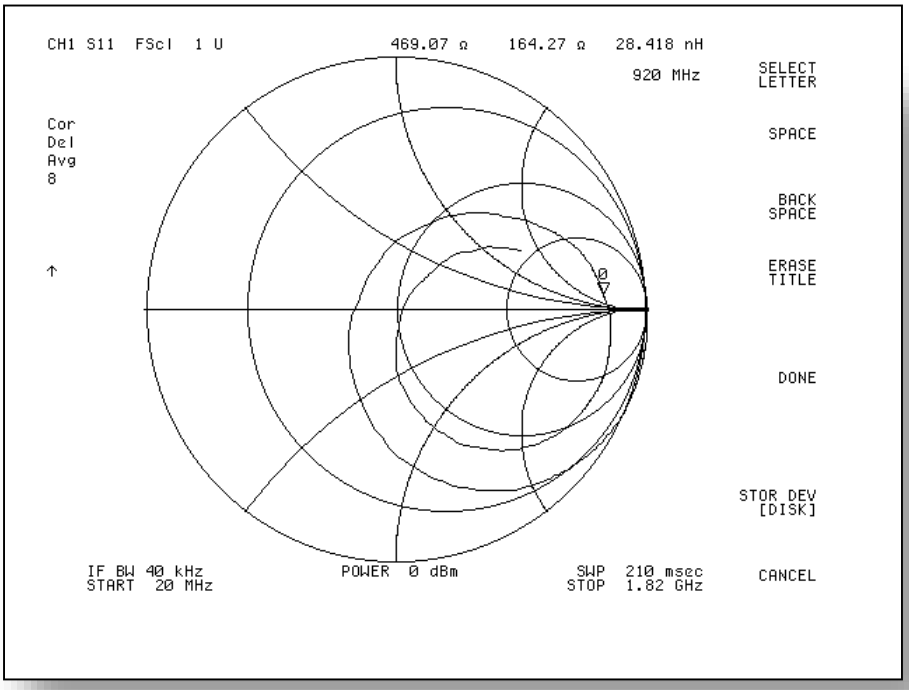

Appendix Figure 6: Smith chart data for 12AWG_130mm Straight monopole antenna

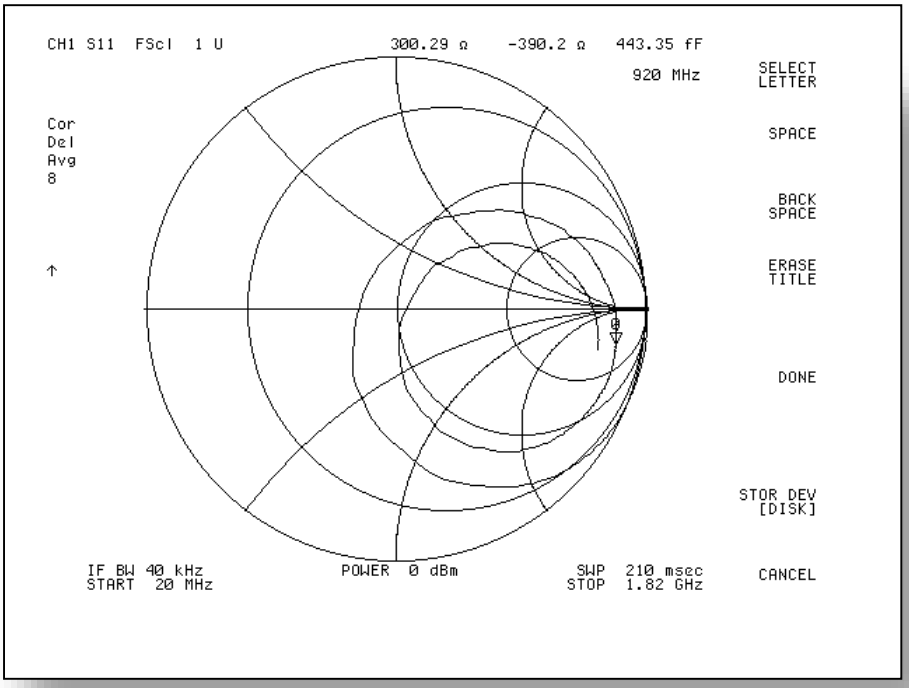

Appendix Figure 7: Smith chart data for 14AWG_161mm Straight monopole antenna

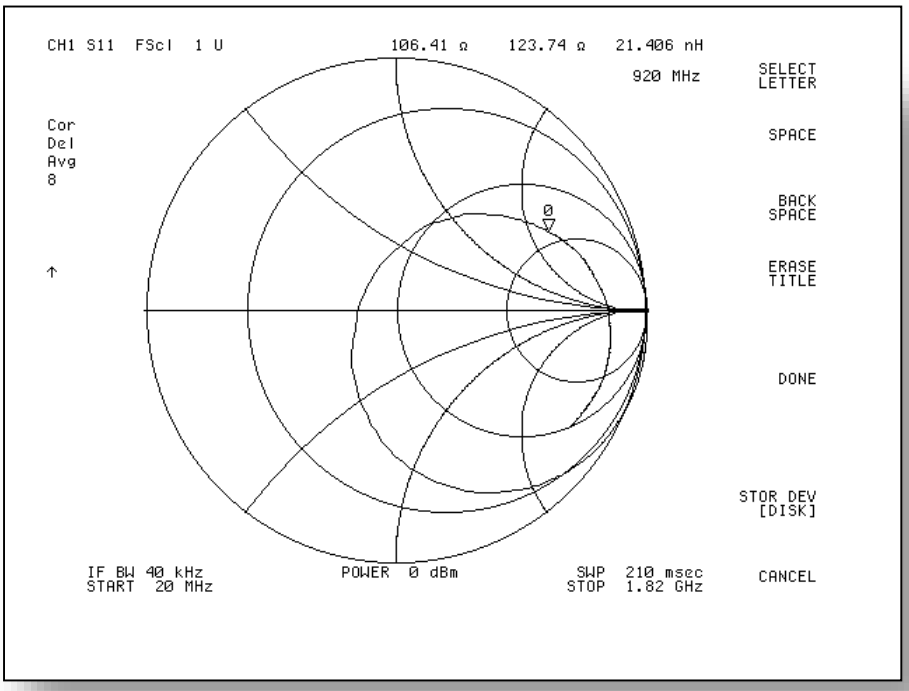

Appendix Figure 8: Smith chart data for 14AWG_100mm Straight monopole antenna